

A study on the eigenanalysis for membranes with stringers using novel  
meshless method in conjunction with SVD and multi-domain techniques,  
respectively  
新型無網格法分別配合奇異值分解法與多重領域分割法兩種技巧分析  
求解含有束制條之薄膜的特徵值問題

K. H. Chen<sup>1</sup> and J. H. Kao<sup>2</sup>

<sup>1</sup> Department of Information Management Toko University Chia-Yi 61363, Taiwan

<sup>2</sup> Department of Harbor and River Engineering National Taiwan Ocean University Keelung  
20224, Taiwan

### Abstract

In this paper, the eigensolutions for membranes with stringers are obtained by using the developed meshless method in conjunction with the SVD technique in a single domain and multi-domain technique in two sub-domains, respectively. The solution is represented by a distribution of double layer potentials. The source points can locate on the real boundary by using the desingularization technique to regularize the singularity and hypersingularity of the kernel functions and the diagonal terms of influence matrices are obtained. The main difficulty of the coincidence of the source and collocation points is disappeared. By adopting the SVD technique for rank revealing, the nontrivial boundary mode are detected by the successive zero singular values which are not due to the degeneracy of degenerate boundary. The boundary modes are obtained according to the right unitary vectors with respect to the zero singular values in the SVD. Finally, the results are compared with the dual boundary element method (DBEM) and it shows the accuracy and efficiency.

**Keywords:** meshless method, SVD, eigensolutions, membranes, multi-domain.

### 摘要

本文中，使用新發展型無網格法並配合奇異值分解法或多重領域分割的技巧，來解含問題具束制條(退化邊界)之薄膜振動問題的特徵值及特徵向量。使用勢能理論的雙層勢能法可將解表現出來。藉由本研究所提出的去奇異技術可將核函數的奇異性與超強奇異性正規化，使得場點與源點可分佈於同一邊界上，因此可解得影響係數矩陣的主對角線上的值。對一含對退化邊界之特徵問題使用無網格法配合奇異值分解法的技巧將可同時省去人工邊界的切割，由奇異值分解法之技巧可得到矩陣的秩降數，藉由考慮不因退化邊界所造成的零奇異值，而可對應到一非無聊解的邊界模態。此邊界模態可依據奇異值分解法中零奇異值所對應的右首向量。最後本法所得之結果與對偶邊界元素法作比較後，驗證了此新型無網格法的精準度與效率。

**關鍵字:** 無網格法，奇異值分解法，特徵解，薄膜，多重領域。

## 1. Introduction

Over twenty years, the main applications were limited in BVPs without degenerate boundaries. Since the degenerate boundary results in rank deficiency for the Meshless method and BEM, the multi-domain BEM [2] was utilized to solve the nonunique solution by introducing an artificial boundary. The drawback of the multi-domain approach is obvious in that the artificial boundary is arbitrary, and thus not qualified as an automatic scheme. In addition, a larger system of equations is required since the degrees of freedoms on the interface are put into the system. For half plane or infinite problem, the artificial boundary is not finite. The three shortcomings encourage us to deal with the degenerate boundary problem by using the single domain concept with SVD technique.

Up to the present, no literature has been published in international journal by using the meshless method [3, 4] without the multi-domain approach to the authors' best knowledge. We may wonder is it possible to find the eigensolution in a single domain with a degenerate boundary approach. Therefore, we deal with the degenerate problem using the novel meshless method in conjunction with the SVD technique in this paper. We solve the membrane eigenproblems with stringers using the novel meshless method+SVD. By employing only the novel meshless method, the eigenvalue is detected in a single domain by finding the successive zero singular values using the rank revealing technique of SVD. The case with inclined stringer is solved.

## 2. Formulation

### 2-1 Formulation of novel meshless method

By employing the RBF technique, the acoustic pressure can be approximated in terms of the strengths of the singularities ( $s^j$ ) as

$$u(x^i) = \sum_{j=1}^N A^I(s^j, x^i) \alpha^j, \quad x \in D^I \quad (1)$$

$$t(x^i) = \sum_{j=1}^N B^I(s^j, x^i) \alpha^j, \quad x \in D^I \quad (2)$$

where  $A^I(s^j, x^i)$  is the RBF in which the superscript,  $I$ , denotes the interior domain,  $\alpha^j$  are the unknown coefficients,  $N$  is the number of source points,  $s^j$ , and  $B^I(s^j, x^i) = \frac{\partial A^I(s^j, x^i)}{\partial n_x}$ . The

coefficients  $\{\alpha^j\}_{j=1}^N$  are determined, such that BC is satisfied at the boundary points ( $\{x^i\}_{i=1}^N$ ). By

collocating  $N$  observation points,  $x^i$ , for the Dirichlet boundary and the Neumann boundary, we have the following  $N \times N$  linear systems in the form of

$$\{\bar{u}^i\} = \{0\} = \begin{bmatrix} a_{1,1} & a_{1,2} & \cdots & a_{1,N} \\ a_{2,1} & a_{2,2} & \cdots & a_{2,N} \\ \vdots & \vdots & \ddots & \vdots \\ a_{N,1} & a_{N,2} & \cdots & a_{N,N} \end{bmatrix} \{\alpha^j\} = [A^I] \{\alpha^j\}, \quad (3)$$

$$\{\bar{T}^i\} = \{0\} = \begin{bmatrix} b_{1,1} & b_{1,2} & \cdots & b_{1,N} \\ b_{2,1} & b_{2,2} & \cdots & b_{2,N} \\ \vdots & \vdots & \ddots & \vdots \\ b_{N,1} & b_{N,2} & \cdots & b_{N,N} \end{bmatrix} \{\alpha^j\} = [B^T] \{\alpha^j\}, \quad (4)$$

where

$$a_{i,j} = A^I(s^j, x^i), \quad i, j = 1, 2, \dots, N \quad (5)$$

$$b_{i,j} = B^I(s^j, x^i), \quad i, j = 1, 2, \dots, N \quad (6)$$

The chosen RBFs are the double layer potentials from the potential theory given as:

$$A^I(s^j, x^i) = -\frac{i\pi k}{2} H_1^{(1)}(kr_{ij}) \frac{n_k y_k}{r_{ij}}, \quad (7)$$

$$B^I(s^j, x^i) = \frac{i\pi k}{2} \left\{ k(H_2^{(1)}(kr_{ij}) \frac{y_k y_l n_k \bar{n}_l}{r_{ij}^2} - H_1^{(1)}(kr_{ij}) \frac{n_k \bar{n}_k}{r_{ij}} \right\}, \quad (8)$$

where  $H_2^{(1)}(kr_{ij})$  is the Hankel function of the first kind and the second order.

$r_{ij} = \sum_{k=1}^2 |s_k^j - x_k^i|$ ,  $y_k n_k = \sum_{k=1}^2 (x_k^i - s_k^j) n_k$ ,  $n_k$  is the  $k$ -th component of the outward normal vector at

source point  $s^j$ ;  $\bar{n}_k$  is the  $k$ -th component of the outward normal vector at field point  $x^i$ . It is noted

that the double layer potentials in Eqs.(7) and (8) have both singularity and hypersingularity at the origin, which leads to troublesome singular kernels and controversial auxiliary boundary for the MFS. The off-set distance between the off-set (auxiliary) boundary ( $B'$ ) and the real boundary ( $B$ ) needs to be chosen deliberately. To overcome this drawback,  $s^j$  is distributed on the real boundary by using the following proposed regularized techniques. The rationale for choosing the double layer potential instead of single layer potential as used in the proposed method for the form of RBFs is to take advantage of the regularization of the subtracting and adding-back technique, so that no off-set distance is needed when evaluating the diagonal coefficients of influence matrices as explaining in the following section. The single layer potential cannot be chosen as the form of RBFs, because the Eqs.(13) and (14) in the following text of next section are not satisfied. If the single layer potential is used, the regularized technique of subtracting and adding-back method will fail [5, 6].

2-2 Derivation of diagonal coefficients of influence matrices for arbitrary domain using a singular meshless method

When the collocation point  $x^i$  approaches to the source point  $s^j$ , Eqs.(7) and (8) will be approximated by:

$$\lim_{x_i \rightarrow s_j} A^E(s^j, x^i) = \bar{A}^E(s^j, x^i) = \frac{n_k y_k}{r_{ij}^2} \quad (9)$$

$$\lim_{x_i \rightarrow s_j} B^E(s^j, x^i) = \bar{B}^E(s^j, x^i) = (2 \frac{y_k y_l n_k \bar{n}_l}{r_{ij}^4} - \frac{n_k \bar{n}_k}{r_{ij}^2}) + \frac{k^2}{4} i, \quad (10)$$

by using the limiting form for small arguments and the identities from the generalized function as shown below [1], where the superscript,  $E$ , denotes the exterior domain,

$$\lim_{r_{ij} \rightarrow 0} H_1^{(1)}(kr_{ij}) = \frac{kr_{ij}}{2} + \frac{2}{\pi kr_{ij}} i, \quad (11)$$

$$\lim_{r_{ij} \rightarrow 0} H_2^{(1)}(kr_{ij}) = \frac{(kr_{ij})^2}{8} + \frac{4}{\pi(kr_{ij})^2} i. \quad (12)$$

The kernels in Eqs.(9) and (10) have the same singularity strength as the Laplace equation [?]. Therefore, Eqs.(1) and (2) for the eigenproblem need to be regularized by using special treatment such as

$$\begin{aligned} \bar{u}(x^i) = 0 &= \sum_{j=1}^N A^I(s^j, x^i) \alpha^j - \sum_{j=1}^N \bar{A}^E(s^j, x^i) \alpha^i \\ &= \sum_{j=1}^{i-1} A^I(s^j, x^i) \alpha^j + \sum_{j=i+1}^N A^I(s^j, x^i) \alpha^j \end{aligned} \quad (13)$$

$$\begin{aligned} & - [\sum_{m=1}^N \bar{A}^E(s^m, x^i) - A^I(s^i, x^i)] \alpha^i, \quad x^i \in B \\ \bar{t}(x^i) = 0 &= \sum_{j=1}^N B^I(s^j, x^i) \alpha^j - \sum_{j=1}^N \bar{B}^E(s^j, x^i) \alpha^i \\ &= \sum_{j=1}^{i-1} B^I(s^j, x^i) \alpha^j + \sum_{j=i+1}^N B^I(s^j, x^i) \alpha^j \end{aligned} \quad (14)$$

$$- [\sum_{m=1}^N \bar{B}^E(s^m, x^i) - B^I(s^i, x^i)] \alpha^i, \quad x^i \in B$$

where  $\bar{A}^E(s^j, x^i)$  and  $\bar{B}^E(s^j, x^i)$  are the double layer potentials of the exterior problem of Laplace equation for the same boundary, in which

$$\sum_{j=1}^N \bar{A}^E(s^j, x^i) = 0, \quad (15)$$

$$\sum_{j=1}^N \bar{B}^E(s^j, x^i) = 0. \quad (16)$$

The original singular terms of  $A^I(s^i, x^i)$  and  $B^I(s^i, x^i)$  in Eqs.(1) and (2), have been transformed into regular terms  $-[\sum_{m=1}^N \bar{A}^E(s^m, x^i) - A^I(s^i, x^i)]$  and  $-[\sum_{m=1}^N \bar{B}^E(s^m, x^i) - B^I(s^i, x^i)]$  in Eqs.(13) and (14), respectively. In which the terms of  $\sum_{m=1}^N \bar{A}^E(s^m, x^i)$  and  $\sum_{m=1}^N \bar{B}^E(s^m, x^i)$  are the adding-back terms and the terms of  $A^I(s^i, x^i)$  and  $B^I(s^i, x^i)$  are the subtracting terms in the two

brackets for the special treatment technique. After using the regularized technique of subtracting and adding-back method [5, 6], we are able to remove the singularity and hypersingularity of the kernel functions. Therefore, the diagonal coefficients for the influence matrices can be extracted out as:

$$\{0\} = \begin{bmatrix} \sum_{m=1}^N \bar{a}_{1,m} - a_{1,1} & a_{1,2} & \cdots & a_{1,N} \\ a_{2,1} & \sum_{m=1}^N \bar{a}_{2,m} - a_{2,2} & \cdots & a_{2,N} \\ \vdots & \vdots & \ddots & \vdots \\ a_{N,1} & a_{N,2} & \cdots & \sum_{m=1}^N \bar{a}_{N,m} - a_{N,N} \end{bmatrix} \{\alpha^j\}, \quad (17)$$

$$\{0\} = \begin{bmatrix} -(\sum_{m=1}^N \bar{b}_{1,m} - b_{1,1}) & b_{1,2} & \cdots & b_{1,N} \\ b_{2,1} & -(\sum_{m=1}^N \bar{b}_{2,m} - b_{2,2}) & \cdots & b_{2,N} \\ \vdots & \vdots & \ddots & \vdots \\ b_{N,1} & b_{N,2} & \cdots & -(\sum_{m=1}^N \bar{b}_{N,m} - b_{N,N}) \end{bmatrix} \{\alpha^j\}. \quad (18)$$

where  $a_{ij} = A^I(s^j, x^i)$ ,  $\bar{a}_{ij} = \bar{A}^E(s^j, x^i)$ ,  $b_{ij} = B^I(s^j, x^i)$ , and  $\bar{b}_{ij} = \bar{B}^E(s^j, x^i)$ . By collocating  $N$  observation points on real boundary to match with the BCs from Dirichlet boundary condition and Neumann boundary condition, we can get the final system of Eqs. (17) and (18).

## 2-3 Treatment of degenerate boundary problems

### (1). Multi-domain technique

For normal boundary problems, the proposed meshless method can be applied directly on them without difficulty. But for degenerate boundary problem, it will encounter rank-deficient problem due to the coincidence of boundary nodes on the degenerate boundary. The general technique to carry out the degenerate boundary problem by the use of dual boundary element method (DBEM), multi-domain BEM [2] is always applicable way to solve it. Here we combine the multi-domain technique and our proposed meshless method to handle it.

According to the concept of multi-domain technique, it separates the domain into  $D^+$  and  $D^-$ , which can be seen in Fig.1, and the labels of subdomains  $D^+$  and  $D^-$  are given  $a$  and  $b$  as subscripts, respectively. Thus the problems need two more constraints on the interface between two subdomains. The additional two constraints of the continuity and equilibrium conditions on the interface are

$\phi_a^* = \phi_b^*$  and  $\psi_a^* = -\psi_b^*$ , where the supscript  $*$  denote the interface. After that, this concept combining

with the above mentioned meshless method can deal with this problem, and it can be implemented as

$$\begin{bmatrix} A_{a,a}^I & A_{a,a^*}^I & 0 & 0 \\ A_{a^*,a}^I & A_{a^*,a^*}^I & -A_{b^*,b^*}^I & -A_{b^*,b}^I \\ B_{a^*,a}^I & B_{a^*,a^*}^I & B_{b^*,b^*}^I & B_{b^*,b}^I \\ 0 & 0 & A_{b,b}^I & A_{b,b^*}^I \end{bmatrix} \begin{Bmatrix} \alpha_a \\ \alpha_a^* \\ \alpha_b^* \\ \alpha_b \end{Bmatrix} = \begin{Bmatrix} 0 \\ 0 \\ 0 \\ 0 \end{Bmatrix} \quad (19)$$

(2) Singular value decomposition technique

(a) *Direct-searching scheme in the novel meshless method*

The eigenvalue  $k$  can be obtained by direct searching the rank versus  $k$ , such that

$$\text{Rank}([A^I]) = N-1, \quad \text{for Dirichlet problem} \quad (20)$$

and

$$\text{Rank}([B^I]) = N-1, \quad \text{for Neumann problem} \quad (21)$$

After determining the eigenvalues, the boundary mode can be obtained by setting a normalized value to be one in a boundary node for the nontrivial vector. By substituting the eigenvalue and boundary mode into Eqs.(1) and (2), the interior mode can be obtained.

(b) *Novel meshless method +SVD*

The aforementioned the multi-domain technique is well known for degenerate boundary problems in the literature. Here, we propose a new approach to deal with the eigenproblem using the novel meshless method in conjunction SVD technique. The sketch of distribution of source points on the degenerate boundary was shown in Fig.2. The influence matrix  $[A^I]$  and  $[B^I]$  are rank deficient due to two sources, the degeneracy of stringers and the nontrivial mode for the eigensolution. Since  $N_d$  is the numbers of source points locate on the stringer, the matrix  $[A^I]$  and  $[B^I]$  result in  $N_d$  zero singular values ( $\sigma_1 = \sigma_2 = \dots = \sigma_{N_d} = 0$ )

The next  $N_d^{\text{th}}$  zero singular value  $\sigma_{N_d+1} = 0$  originates from the nontrivial eigensolution. To detect the eigenvalues, the  $\sigma_{N_d+1}$  zero singular value versus  $k$  can be plotted to find the drop where the eigenvalue occurs. Since the SVD technique is adopted for rank revealing, the decomposition is reviewed as follow:

Given a matrix  $[K]$ , SVD can decompose into

$$[K(k)]_{M \times P} = [\Phi]_{M \times M} [\Sigma]_{M \times P} [\Psi]_{P \times P}^H \quad (22)$$

where  $[\Phi]$  is a left unitary matrix constructed by the left singular vectors ( $\{\phi_i\}, i = 1, 2, \dots, M$ ), and  $[\Sigma]$  is a diagonal matrix which has singular values  $\sigma_1, \sigma_2, \dots, \sigma_p$  allocated in a diagonal line as

$$[\Sigma]_{M \times P} = \begin{bmatrix} \sigma_p & \dots & 0 \\ \vdots & \ddots & \vdots \\ 0 & \dots & \sigma_1 \\ \vdots & \ddots & \vdots \\ 0 & \dots & 0 \end{bmatrix}_{M \times P}, \quad (23)$$

in which  $\sigma_p \geq \sigma_{p+1} \geq \dots \geq \sigma_1$  and  $[\Psi]_{P \times P}^H$  is the complex conjugate transpose of a right unitary matrix with dimension  $P \times P$  constructed by the right singular vectors ( $\{\psi_i\}, i = 1, 2, \dots, P$ ). As we can see in Eq.(36), there exist at most  $P$  nonzero singular values. By employing the SVD technique to determine the eigenvalue, we can obtain the boundary mode at the same time by extracting the right singular vector  $\{\psi\}$  in the right unitary matrix  $[\Psi]_{P \times P}$  of SVD with respect to the near zero or zero singular value by using

$$[K]\{\psi_i\} = \sigma_i \{\phi_i\}, \quad i = 1, 2, \dots, P. \quad (24)$$

If the  $q^{\text{th}}$  singular value,  $\sigma_q$ , is zero, in Eq.(24) we have

$$[K]\{\psi_q\} = 0\{\phi_q\} = 0, \quad q \leq P. \quad (25)$$

According to Eq.(25), the nontrivial boundary mode is found to be the right singular vector,  $\{\psi_q\}$ , in the right unitary matrix. Therefore, the step to determine nontrivial boundary mode in the multi-domain technique is avoided by setting a reference value. Here, Novel meshless method+SVD employed the influence  $[A']$  or  $[B']$  for  $[K]$  in Eq.(17) for Dirichlet eigenproblem and Eq.(18) for Neumann eigenproblem.

### 3. A benchmark test

The problem are illustrated in Fig.3(a). A square membrane is given with a length  $a$ . For simplicity, we set  $l=1$   $m$ . In this paper, the novel meshless method in conjunction with SVD is employed. In order to check the validity, the results of our proposed meshless method + SVD are compared with DBEM. The distribution of source point for the case is shown in Fig.3(b). Using the proposed method in conjunction with SVD, the  $(\sigma_{N_d+1})^{\text{th}}$  zero singular value obtained by using

Eq.(25) for  $[A']$  matrix, ( $[K] = [A']$ ) is plotted versus the wave number in Fig.4(a). The

curve drops at the eigenvalues. Direct searching scheme to extract out true and spurious eigenvalues resulted from degenerate boundary and nontrivial solution is employed in the present paper. For the generalized algebraic eigenproblem, some effective schemes have been proposed, e.g. William-Wellie algorithm. Since this is not our main focus, the efficient algorithm is not discussed here. By using the dual BEM, the determinants versus the wave number are also shown in Fig.4(b). Good agreements for the former eigenvalues are made. For this case, the number of boundary nodes,  $N_d$ , on the degenerate

boundary is 10. Since the  $(N_d + 1)^{\text{th}}$  zero singular value,  $(\sigma_{N_d+1})^{\text{th}}$ , originates from the nontrivial boundary mode, Fig.5(a) shows the  $\psi_{N_d+1}$  along the boundary for the solved unknown densities

corresponding to the former four eigenvalues. For the former four eigenvalues, the first right singular vector  $\psi_1$  corresponding to the first zero singular value ( $\sigma_1 = 0$ ) along the boundary in Fig.5(b), also indicate that the  $\psi_1$  is trivial except on the degenerate boundary. Since the former  $N_d$  zero singular

values ( $\sigma_1 = \sigma_2 \cdots = \sigma_{N_d} = 0$ ) originate from the degenerate boundary, the corresponding right singular vectors ( $\psi_1 \sim \psi_{N_d}$ ) are found to be trivial except on the degenerate boundary as shown in Fig.6, for the case of  $k=4.6$ . In other words, Fig.6 reveals that the former ten zero singular values stem from the degeneracy due to stringer. The former four modes are compared well with those of DBEM as shown in Fig.7(a) and (b).

#### 4. Conclusions

Instead of using the conventional meshless method in conjunction with multi-domain technique, the novel meshless method was successfully utilized to solve the degenerate boundary eigenproblem in conjunction with the SVD technique. Not only the drawback of conventional MFS can be avoided but also a single domain is required. By detecting the successive zero singular values, the eigenvalues were found and the boundary eigenmodes were obtained according to the corresponding right unitary vectors. Good agreement between the results of present method and the dual BEM was obtained. The goal to solve the eigenproblem using the singular formulation in a single domain was achieved. In addition, the boundary mode and eigenvalue can be obtained at the same time once the influence matrix was decomposed by using the SVD.

#### Acknowledgement

Financial support from the National Science Council under Grant No. NSC-94-2211-E-464-002 for Toko University is gratefully acknowledged.

#### REFERENCES

- [1] M. Abramowitz, I. A. Stegun, Handbook of mathematical functions with formulation graphs and mathematical tables, New York, Dover, 1972.
- [2] J. T. Chen, S. R. Lin, K. H. Chen and S. W. Chyuan, Eigenanalysis for membranes with stringers using conventional BEM in conjunction with SVD technique, Computer Methods in Applied Mechanics and Engineering, 192 (11-12) 2003 1299-1322
- [3] W. Chen, M. Tanaka, A meshfree, integration-free and boundary-only RBF technique, Comput. Math. Appl. 43 2002 379-391.
- [4] G. Fairweather, A. Karageorghis, The method of fundamental solutions for elliptic boundary value problems, Adv. Comput. Math. 9 1998 69-95.
- [5] D. L. Young, K.H. Chen, C.W. Lee, Novel meshless method for solving the potential problems with arbitrary domains, J. Comput. Phys. 209 2005 290-321.
- [6] D. L. Young, K.H. Chen, C.W. Lee, Singular meshless method using double layer potentials for exterior acoustics, J. Acoust. Soc. Am., 119(1) 2006 96-107.

Figures

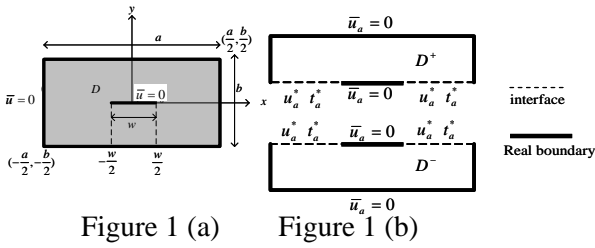


Figure 1 (a) Figure 1 (b)

Figure 1 (a) Sketch of degenerate boundary problem (b) the scheme of multi-domain technique.

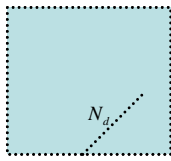


Figure 2 Sketch for the distribution of source points on the degenerate boundary.

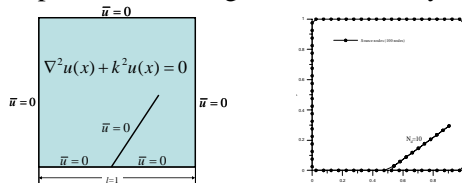


Figure 3 (a) Figure 3 (b)

Figure 3 The benchmark case of (a) Sketch of degenerate boundary problem, (b) The distribution of source point.

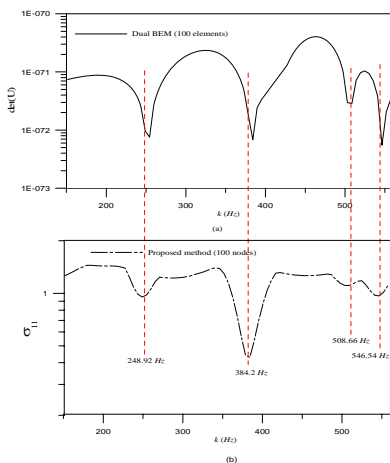


Fig. 4 (a) The  $(\sigma_{N_d+1})$ th zero singular value versus the wave number using the novel meshless method+SVD. (b) The determinant versus the wave number using the dual BEM.

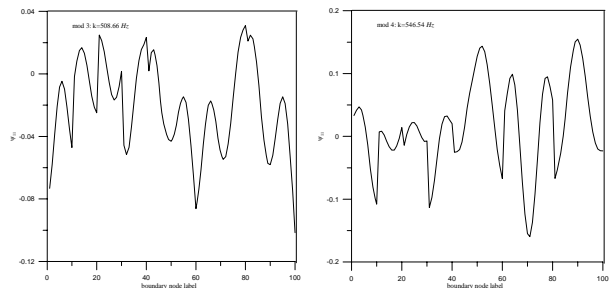
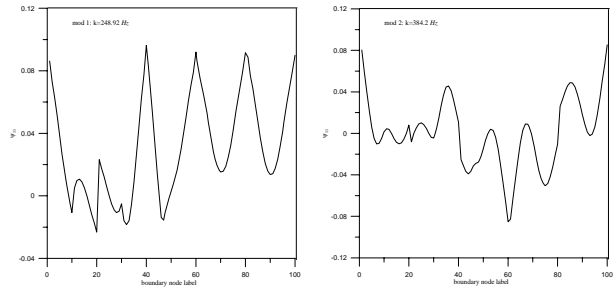


Figure 5 (a)

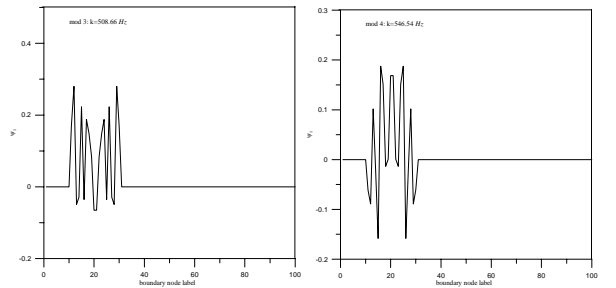
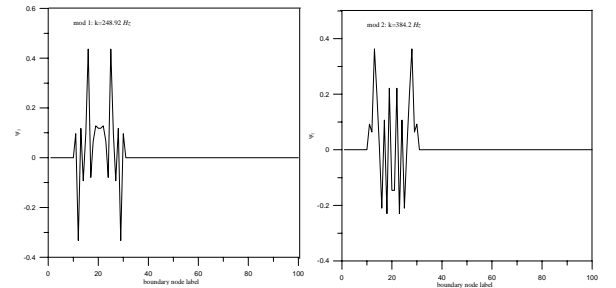


Figure 5 (b)

Figure 5 (a) The solved unknown densities,  $\psi_{N_d+1} = \psi_{11}$ , along the boundary (1–10, degenerate boundary, 11–70, normal boundary) for the former four eigenvalues. (b) The boundary eigensolution  $\psi_1$  along the boundary

(1-10, degenerate boundary, 11-100, normal boundary) for the former four eigenvalues.

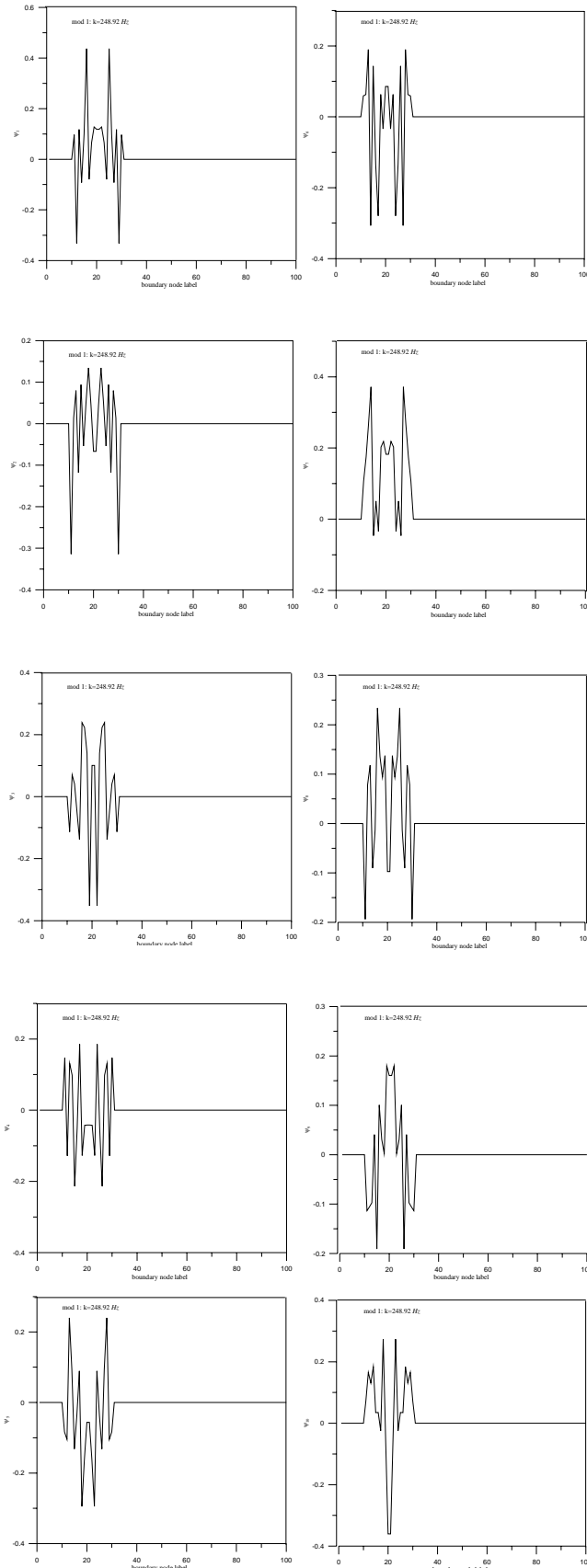


Figure 6 The right singular vectors ( $\psi_1 \sim \psi_{10}$ ) corresponding the former ten zero singular values for the case of mode1(k=248.92 Hz).

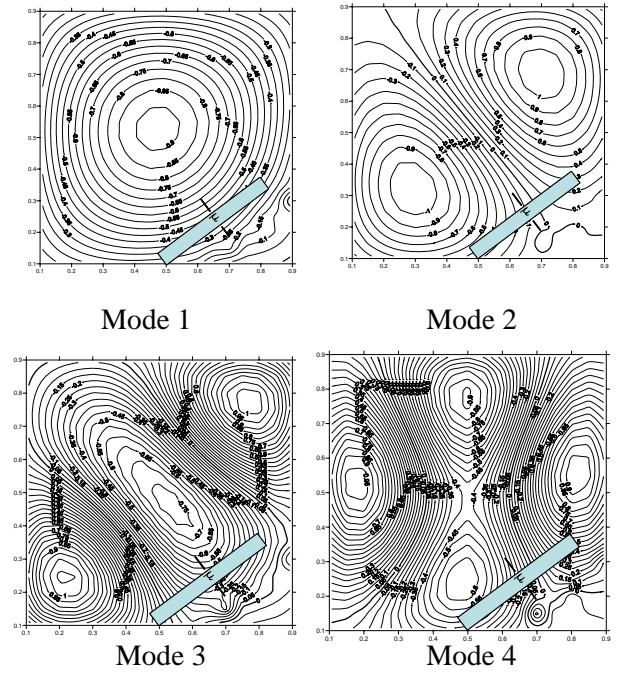


Figure 7 (a)

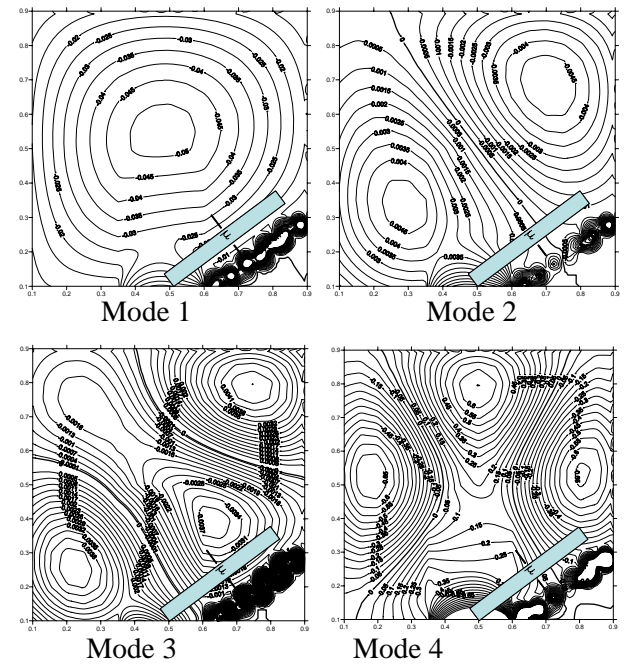


Figure 7(b)

Figure 7 The former four modes, (a) The proposed meshless method + SVD, (b) DBEM